High Voltage

Research Article

IET Journals
The Institution of Engineering and Technology

Series LC DC circuit breaker

eISSN 2397-7264
Received on 8th January 2019
Revised 26th March 2019
Accepted on 1st April 2019
E-First on 30th April 2019
doi: 10.1049/hve.2019.0003
www.ietdl.org

Dragan Jovcic[1] ✉

[1]*School of Engineering, University of Aberdeen, AB24 3UE, Aberdeen, UK*
✉ *E-mail: d.jovcic@abdn.ac.uk*

Abstract: The article proposes a mechanical DC circuit breaker (CB) based on a series LC circuit. It requires two switches (a fast disconnector and an AC circuit breaker), an inductor and a capacitor, and therefore the cost is expected to be low. A series LC circuit is analysed and it is concluded that fault current will always have natural zero-current crossings which enable use of simple AC CBs. The current commutation into a capacitor is investigated since this is important for successful operation. A number of analytical conditions are derived for the voltage stress across disconnector contacts which enable arc-less contact opening. Experimental results on a 900 V laboratory prototype LC DC CB illustrate successful DC fault clearing, with commutation of 130 A and peak DC current of 190 A. A detailed PSCAD model for 320 kV LC DC CB is developed and DC fault clearing is evaluated in order to understand the possible benefit for high-voltage direct current applications. Further comparisons with the commercialised hybrid DC CB and mechanical DC CB on 320 kV system illustrate some benefits in terms of performance and simplicity. The mechanical LC DC CB operates very fast because of early capacitor insertion, and this results in low peak current and energy dissipation.

1 Introduction

There is significant interest to advance high-voltage direct current (HVDC) transmission technology into multi-terminal DC and DC grids worldwide [1]. There are multiple technical, operational and cost-related difficulties to achieve this goal, but the lack of DC circuit breaker (CB) with acceptable performance and affordable costs is the most prominent technical challenge. Additionally, cost-effective DC CB would bring significant benefits in many other DC systems in industry at medium DC voltage level.

Some of the main challenges with DC faults are [2, 3]:

i. DC fault current has no zero crossings which imply that conventional AC CBs cannot be used. More complex devices are required.
ii. DC fault current will rise to very high values in short time. Fast operating speed (i.e. few milliseconds) is an essential requirement for DC CBs.
iii. DC CBs will require large energy absorbers, which add to DC CB size, weight and cost.

Different DC CB technologies (i.e. solid state, mechanical, and hybrid) have been developed and high-voltage prototypes demonstrated [4–8].

The first generation of DC CBs employed conventional AC interrupters with a passive resonant circuit which generally required quite long arcing of 10–50 ms before interruption [4]. A faster mechanical DC CB with opening time of around 8 ms has also been developed recently and demonstrated as high-voltage prototype [5]. It requires two vacuum AC CBs with fast driving mechanism, and employs pre-charged capacitor. These mechanical topologies generally lead to dissipation of large amount of DC fault current energy, which may reach 30–70 MJ.

The hybrid IGBT-based DC CB [7], is the fastest operating technology, where opening time is specified as 2 ms (time for DC voltage to recover and time to peak current). It also provides low-loss operation in closed state. However, high voltage and current rating for semiconductor valves is the main disadvantage of this DC CB. A unidirectional version requires a semiconductor valve rated for full DC voltage, while bidirectional version will require two such valves which are like valves used in HVDC converters. The energy dissipation will amount to 10–30 MJ for a typical 320 kV device, which implies large energy absorbers.

The hybrid thyristor-based DC CB [8] is also developed to high-voltage prototype and uses similar topology as IGBT-based hybrid DC CB. It has some advantages of higher current capability and perhaps lower costs, but essentially suffers all shortcomings mentioned with IGBT topology.

The fastest hybrid DC CBs may not be sufficiently fast to avoid converter blocking in case of DC faults. Assuming 2.5 ms total time between fault initiation and peak fault current, the peak current will reach at least 6 kA before the fault is isolated, and this will cause (temporary) blocking of modular multilevel converter HVDC converters. This may become important drawback in DC grid development, since system reliability aspects will be crucial as DC grid grows into very large size.

The cost of DC CB is not known. However, the cost of traditional AC vacuum switches is understood to be much lower than a comparable HV valve used in HVDC [9]. This gives incentive for researching further fully mechanical DC CB topologies.

The high-speed mechanical switches have been known for many years [10–12]. They normally employ Thomson coils which provide very high initial force to enable contact acceleration. Similar high-speed technology has been used for disconnectors and for circuit breakers. Circuit breakers have arc-sustaining contacts which are heavy and require high driving force, thus lowering operating speed.

High-speed disconnectors have the best prospects of achieving required opening speeds at low costs. Nevertheless, the current breaking capability of disconnectors is minimal, and, as an example, it is listed as 1 A in [13, 14]. A very similar device is also employed by another manufacturer [15].

This research proposes to improve speed of DC fault isolation, by exploiting voltage withstand of fast disconnectors while their contacts are on the move. This new method postulates that a disconnector can insert a series capacitor to convert DC to AC, while another conventional AC CB can interrupt the AC current. The goal is to develop a mechanical DC CB topology with high performance and acceptable costs. Theoretical and simulation methods will be used to develop the design method, while low-voltage experimental approach will verify the concept.

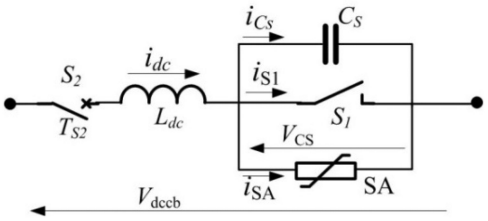

Fig. 1 *Schematic of series LC DC CB*

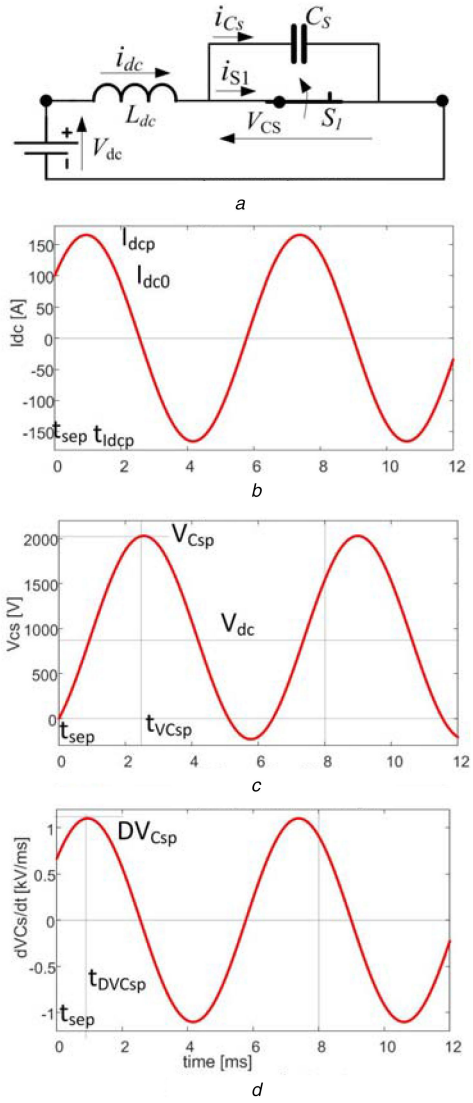

Fig. 2 *Series LC circuit and response when S_1 opens*

(a) Circuit diagram, ***(b)*** Load current, ***(c)*** Capacitor voltage, ***(d)*** Voltage derivative

2 Series LC DC CB

Fig. 1 shows schematic of proposed LC DC CB. It includes:

- Fast mechanical switch S_1, which can be high-speed disconnector. Fast operating speed brings benefits in terms of size, weight and costs of other components.
- Mechanical switch S_2, which is a standard AC CB. Enhanced operating speed brings some benefits.
- Inductor L_{dc} for limiting initial current rise and for creating LC resonance with C_s capacitor.
- Capacitor C_s for limiting voltage gradient while S_1 contacts are separating, and for creating zero-crossings by series LC network with inductor L_{dc}.

The proposed DC CB consists solely of mechanical components which brings cost advantages. Furthermore energy absorber may not be essential, or if used a modest capacity is needed. Capacitor is the most expensive component, but examples further below indicate that the practical value of capacitance is acceptable.

The CB opening process (DC current interruption) is summarised as follows:

i. S_1 and S_2 are closed and the ON state losses are negligible. Capacitor C_s is discharged since S_1 is closed. On receiving DC CB trip signal the S_1 switch is commanded to open immediately. In a short time S_1 contacts begin to separate.
ii. While S_1 contacts gap increases, the load current charges capacitor C_s. Due to relatively large L_{dc} and C_s, the capacitor voltage will be stable and can be readily estimated using LC circuit theory. At any instant while contacts are moving, the capacitor voltage should be below the voltage withstand capability of S_1. It will be shown that this can be achieved with common disconnector designs. In fully open state S_1 is stressed to the peak capacitor voltage.
iii. Once S_1 is open the series LC circuit converts DC current into AC current. After C_s is inserted in series, S_2 experiences only AC current which has natural zero-crossings and can be easily interrupted. S_2 open signal is timed considering switch speed, and to reduce arcing. S_2 contacts separate, temporary arc is formed as in all AC CBs, and current is interrupted at the next zero crossing.
iv. At this stage the fault current is interrupted, but capacitor Cs is charged. The next closing process can begin with a charged capacitor, as an example if closing of S_1 is timed with zero voltage on Cs on the oscillating voltage waveform. Alternatively, C_s can be simply discharged with an external resistor.

The closing process is not analysed in depth, but it is normally not a big challenge even for high voltage DC circuits. If S_1 is closed, S_2 can readily close even under load current. Alternatively, S_2 is firstly closed and then S_1 is closed on the exact point of AC voltage V_{C_s} to avoid arcing.

3 Background on series LC circuit

Fig. 2*a* shows a simple series LC circuit assuming that switch S_1 is initially closed. The waveforms are shown for the experimental tests system data used later in the paper, and all parameters are given in the appendix. The initial current is $I_{dc0} = 100$ A. Assuming that initially closed S_1 opens at $t = t_{sep}$, the line current and capacitor voltage are shown in Figs. 2*b* and *c*. Also, the voltage derivative is of importance and it is illustrated in Fig. 2*d*. These variables are analytically described by the following formulae:

$$I_{dc} = I_{dco}\cos(\omega_0(t - t_{sep})) + \frac{V_{dc}}{Z_0}\sin(\omega_0(t - t_{sep})) \quad (1)$$

$$V_{C_s} = V_{dc} - V_{dc}\cos(\omega_0(t - t_{sep})) + Z_0 I_{dco}\sin(\omega_0(t - t_{sep})) \quad (2)$$

where $\omega_0 = 2\pi f_0 = 1/\sqrt{L_{dc}C_s}$, $Z_0 = \sqrt{L_{dc}/C_s}$, and I_{dc0} is the initial value of I_{dc}, at $t = t_{sep}$.

The first and second derivatives of the voltage in (2) are

$$\frac{dV_{C_s}}{dt} = \omega_0 V_{dc}\sin(\omega_0(t - t_{sep})) + \omega_0 Z_0 I_{dc0}\cos(\omega_0(t - t_{sep})) \quad (3)$$

$$\frac{d^2V_{C_s}}{dt^2} = \omega_0^2 V_{dc}\cos(\omega_0(t - t_{sep})) - \omega_0^2 Z_0 I_{dc0}\sin(\omega_0(t - t_{sep})) \quad (4)$$

The key values of importance are:

Peak current I_{dcp} and instant of occurrence t_{IDCP}:

$$I_{\mathrm{dcp}} = \sqrt{I_{\mathrm{dc0}}^2 + V_{\mathrm{dc}}^2/Z_o^2}, \quad \tan\left(\omega_0\left(t_{\mathrm{Idcp}} - t_{\mathrm{sep}}\right)\right) = \frac{V_{\mathrm{dc}}}{I_{\mathrm{dc0}}Z_0} \tag{5}$$

Peak voltage V_{Csp} and instant of occurrence t_{VCs}:

$$V_{\mathrm{Csp}} = V_{\mathrm{dc}} + \sqrt{V_{\mathrm{dc}}^2 + I_{\mathrm{dc0}}^2 Z_0^2}, \quad \tan\left(\omega_0\left(t_{\mathrm{Vcsp}} - t_{\mathrm{sep}}\right)\right) = -\frac{I_{\mathrm{dc0}}}{V_{\mathrm{dc}}}Z_0 \tag{6}$$

Peak voltage derivative $\mathrm{DV}_{\mathrm{Csp}}$ and instant of occurrence t_{DVCs}:

$$\mathrm{DV}_{\mathrm{Csp}} = \omega_0\sqrt{V_{\mathrm{dc}}^2 + I_{\mathrm{dc0}}^2 Z_0^2}, \quad \tan\left(\omega_0\left(t_{\mathrm{DVcsp}} - t_{\mathrm{sep}}\right)\right) = \frac{V_{\mathrm{dc}}}{I_{\mathrm{dc0}}Z_0} \tag{7}$$

There are several properties of this circuit which are of importance for DC CB application:

i. Opening S_1 DC circuit converts into AC circuit. A common mechanical AC CB could be used as S_2.
ii. As seen in (1), average value of line current is zero, implying that current zero crossings are certain, and energy dissipation at interruption might be low.
iii. Series capacitor is very effective in reducing the peak current magnitude. Peak current and peak voltage remain constant in the oscillating cycles, and can be managed with selection of L_{dc} and C_{s}.
iv. Low current can also be interrupted. As seen in (1) oscillating current is created even for $I_{\mathrm{dc0}} = 0$.
v. The operating speed is high since the current limiting process starts as soon as capacitor voltage begins to rise.

The peak voltage is of the most significance for the switch S_1 design, while the peak current has most significant impact on the DC grid. Fig. 3 shows the peak voltage $V_{\mathrm{cp}}/V_{\mathrm{dc}}$ and peak current $I_{\mathrm{dcp}}/I_{\mathrm{dc0}}$, depending on Z_0, where $Z_0 = 1$ corresponds to the base case in Fig. 2.

4 Current commutation from switch to a capacitor

4.1 Essential design condition

An important aspect of the DC CB design is the capability to commutate current from the switch S_1 to the capacitor C_{s}.

The withstand (or breakdown) voltage across contacts v_{br} is assumed linearly proportional to the contact separation z, at any instant while contacts are moving $0 < z < z_{\max}$:

$$v_{\mathrm{br}} = zd, \quad 0 < z < z_{\max} \tag{8}$$

where d is the dielectric strength of gap medium, which for air is $d_{\mathrm{air}} = 3$ kV/mm, while for SF6 it is $d_{\mathrm{SF6}} = 7.5$ kV/mm [16]. $z_{\max}$ is the maximum contact distance achieved at time $t_{\max}$. In order to avoid strike at any point while contacts are moving, the following essential condition should be satisfied:

$$zd > v_{\mathrm{cs}}, \quad 0 < z < z_{\max} \tag{9}$$

where capacitor voltage v_{Cs} is assumed identical to the gap voltage. The actual voltage waveform v_{Cs} is the complex expression in (2). The contact distance z will be another complex trajectory which depends on the chosen switch S_1. Some simplifications will be assumed in order to derive practical design conditions. There is no need to consider thermal aspects since no notable arcing is occurring.

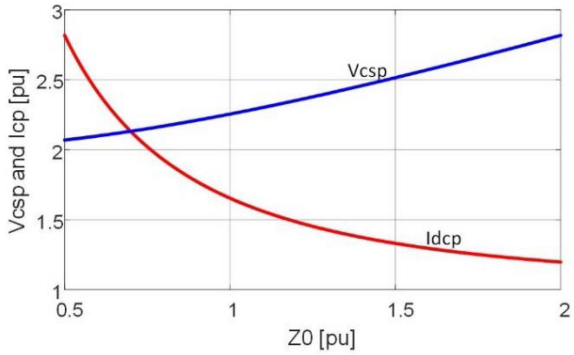

Fig. 3 *Peak voltage and current depending on Zo*

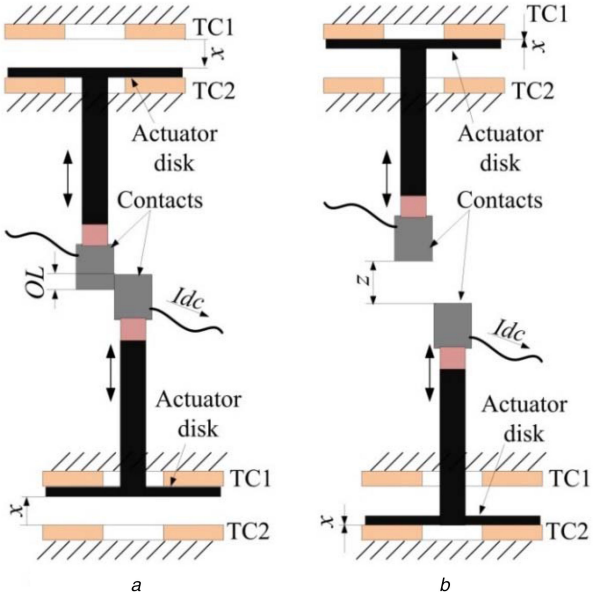

Fig. 4 *Structure of a high-speed switch with lateral contact overlap*
(a) closed position, ***(b)*** Open position

4.2 Final voltage condition

The first design condition is obtained assuming that capacitor voltage at maximum separation distance is adequate:

$$dz > v_{\mathrm{Cs}}, \quad z = z_{\max},\ t = t_{\max} \tag{10}$$

For a given S_1, $z_{\max}$ and $t_{\max}$ will be known and (10) can be used to obtain initial values for L_{dc} and C_s. However (10) would assume an average voltage gradient, and therefore it is not sufficient condition to satisfy (9) for any z.

4.3 Topology for considered switch S_1

From this point it will be assumed that S_1 is a disconnector of a common design topology which is shown in simplified diagram in Fig. 4. Some conventional disconnectors, SF_6 switches and oil switches have such design [13, 17–20], which is characterised by lateral contact overlap in closed state. The lateral overlap, denoted as OL, implies that contacts will accelerate to a non-zero velocity at the separation instant. Considering topology in Fig. 4 the contact separation distance z is determined using the absolute contact position x:

$$z = 2x - \mathrm{OL} \tag{11}$$

A high-speed switch will be commonly driven by a pair of Thomson coils, as shown in Fig. 4, which provide fast acceleration, but only an initial pulse of driving force. Therefore, and considering studies in [13, 17], the following two assumptions can be accepted:

- maximum contact velocity is achieved before contacts separate,
- contact velocity remains constant after separation v = const.

For a given S_1 the contact velocity v will be known.

4.4 Condition at contact separation

At $z = 0$, (9) is difficult to analyse because of singularity. To facilitate design around singularity point, (9) is expressed using contact velocity v, and voltage derivative from (3):

$$d\int_{t_{sep}}^{t} v\,\mathrm{d}t > \int_{t_{sep}}^{t}\left(\frac{\mathrm{d}V_{Cs}}{\mathrm{d}t}\right)\mathrm{d}t, \quad t_{sep} < t < t_{max} \tag{12}$$

The above equation is valid for any final time t including instant of contact separation $t = t_{sep}$. Replacing $t = t_{sep}$ in (12):

$$v\,d > \frac{\mathrm{d}V_{cs}}{\mathrm{d}t}, \quad z = 0,\ t = t_{sep} \tag{13}$$

An observation is made firstly that the capacitor voltage derivative may not be zero at the instant of contact separation, as seen in (3) and in Fig. 2*d*. Replacing (3) in (13) for $t = t_{sep}$, the second necessary condition for arc-less commutation is

$$v\,d > I_{dc0}/C_s, \quad z = 0,\ t = t_{sep} \tag{14}$$

In practical terms, the contact velocity at separation determines current I_{dc0} that can initiate commutation to C_s.

4.5 Average voltage gradient condition

The above two conditions: (10) and (14) are not sufficient to satisfy (9). This is concluded considering that capacitor voltage derivative $\mathrm{d}V_{cs}$ has a peak value in interval $t_{sep} < t < t_{max}$, and it initially increases as seen from the sign of the second derivative in (4) and from Fig. 2*d*. A sufficient but conservative condition to satisfy (9) is to assume that voltage has constant gradient equal to peak voltage derivative obtained in (7). This leads to a simple conservative condition:

$$v\,d > \omega_0\sqrt{V_{dc}^2 + I_{dc0}^2 z_0^2}, \quad 0 < z < z_{max},\ 0 < t < t_{max} \tag{15}$$

A more accurate condition for (constant) voltage gradient can be obtained by averaging (12) in the interval between separation and the peak of the first derivative: $t_{sep} < t < t_{DVdcp}$. This condition can be obtained using (2), (7) and (12):

$$v\,d > \frac{V_{cs}}{t_{DVdcp}}, \quad t = t_{DVdcp} \tag{16}$$

5 900 V LC DC CB experimental verification

5.1 Experimental circuit

The DC CB testing circuit at Aberdeen laboratory has been used previously for testing hybrid and mechanical DC CBs and is described in [17, 21]. It controls DC voltage to 900–1000 V, and supplies fault current of over 500 A.

Fig. 5 shows the experimental LC DC CB. The high-speed disconnector operates in around 2 ms with 3 mm separation in air, and it is described in [17, 22]. Copper contacts of 20 mm width are used, while the closed-state overlap is OL = 1.5 mm. Thomson coils are described in [17], and they provide maximum contact velocity of 2 m/s achieved just before the contacts separate, around 400 µs after the trip signal. This disconnector is capable of interrupting only around 0.5 A DC current at voltages over 100 V.

The switch S_2 is a commercial 900 V Kilovac AC contactor, which has opening time of around 3.2 ms. All the parameters for the experimental DC CB are presented in Table 1. The measuring equipment is:

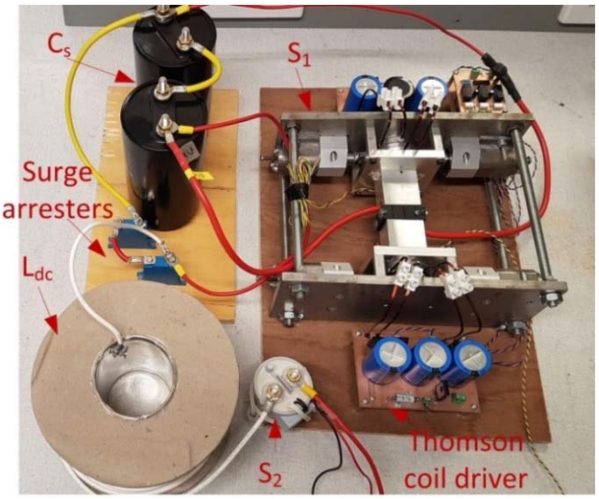

Fig. 5 *Experimental 900 V LC DC CB*

Table 1 Parameters of the 900 V, 200 A, LC DC CB

Parameter	Value	description
V_{dc}	900 V	
I_{dcn}	30 A	
t_{max}	2 ms	in house built high-speed disconnector [17]
OL	1.5 mm	
dielectric stress (air)	0.5 kV/mm	
Z_{max}	3 mm	
L_{dc}	6.8 mH	6 mm^2, 100 m, 77 mm core, 14 × 18
C_s	160 µF	2x Cornell Dubilier 320 µF, 1.2 kV
S2	900 V	Kilovac EV200HAANA
SA	1.1 kV	2x EPCOS, B40K250

- The contact position x is measured using a hall-effect sensor. Contact separation z is estimated using (11). Separation velocity is estimated by differentiating z.
- Currents are measured using Agilent, 2 MHz, 500 A DC probes,
- Voltages are measured using TESTEC, 100 MHz, differential probes.

Data is captured over 8 ms on Agilent 200 MHz oscilloscope. The time is synchronised with S_1 trigger.

5.2 Testing current commutation into capacitor

In order to confirm the commutation principle from a switch into a capacitor a simple experimental circuit is created as shown in Fig. 6*a*. A 10 A current source is shorted with S_1 switch from the experimental set-up in Fig. 5 which receives trip at $t = 0$. The capacitor voltage is a straight line in this case and therefore the conditions (10), (14) and (16) give the same result: C_s>1.8 µF. To ensure adequate safety margin, C_s = 10 µF is selected.

The circuit currents are shown in Fig. 6*b*, and the conclusion is that the switch current I_{S1} rapidly reduces to zero, while the main current is commutated to capacitor.

Fig. 6*c* shows that the capacitor voltage rises fast and no arcing is present. Fig. 6*d* illustrates that the measured contact velocity is around 2 m/s at separation, which remains constant. After commutation, it is seen that the power supply reduces current because of overvoltage protection, but this does not negate validity of conclusions.

5.3 Testing DC fault current interruption

The value for inductance L_{dc} = 6.8 mH is determined firstly considering that trip signal is sent at I_{dc} = 40 A and desired initial

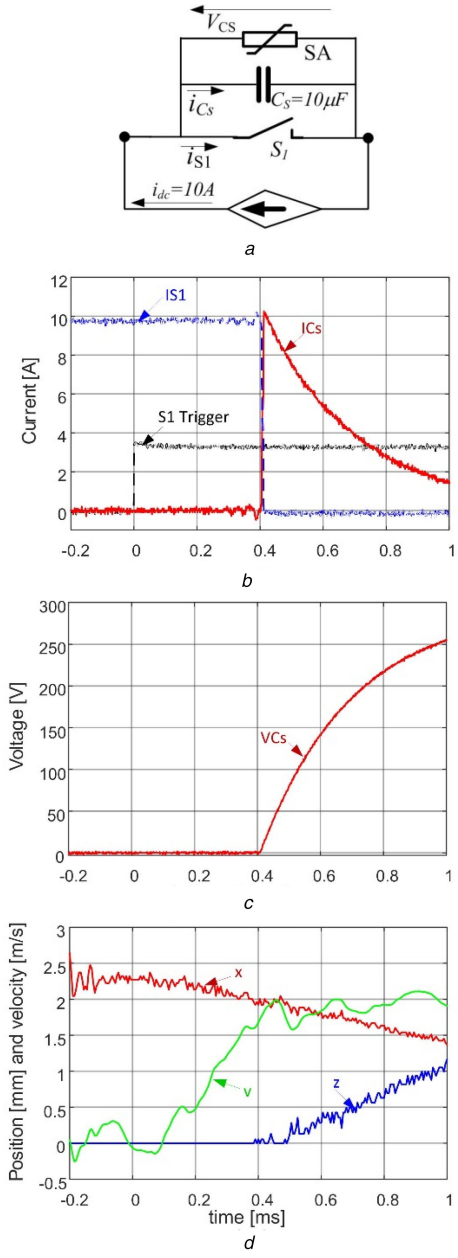

Fig. 6 *Commutation from switch S_1 into a capacitor*

(a), ***(b)*** Source and S_1 currents, ***(c)*** Capacitor voltage, ***(d)*** Switch S_1 contact position and velocity

current is $I_{dc0} = 130$ A. The condition (14) gives $C_s > 22$ μF, while (15) gives $C_s > 24$ μF. To account for parasitic impedances and to provide consistent safety margin (at $z_{max} = 3$ mm, $V_{max} = 1.3$ kV) $C_s = 160$ μF is selected.

Fig. 7 shows the experimental results for clearing a DC fault. The initial load current is around 5 A, and fault is detected when $I_{dc} > 40$ A. It is seen in Fig. 7*c* that it takes around 150 μs for contacts to start moving, while separation occurs at $t = 400$ μs. Also, the velocity at separation is $v = 2$ m/s ($t = t_{sep}$) which then remains constant. The speed increase at the very end of travel is a consequence of bi-stable springs.

Fig. 7*b* shows the S_1 switch current, capacitor current and DC line current. It is observed that 130 A is commutated from S_1 to C_s instantaneously and without arcing. Many further tests have been performed and no arcing or contact deformation is observed. However no tests are done to optimise capacitance to a smaller value. The DC current is interrupted at first zero crossing (at 4.5 ms) by contactor S_2.

Fig. 7*a* shows that capacitor voltage rises to 1150 V in 1.5 ms, and it is limited by the arresters. The switch S_2 is timed in order

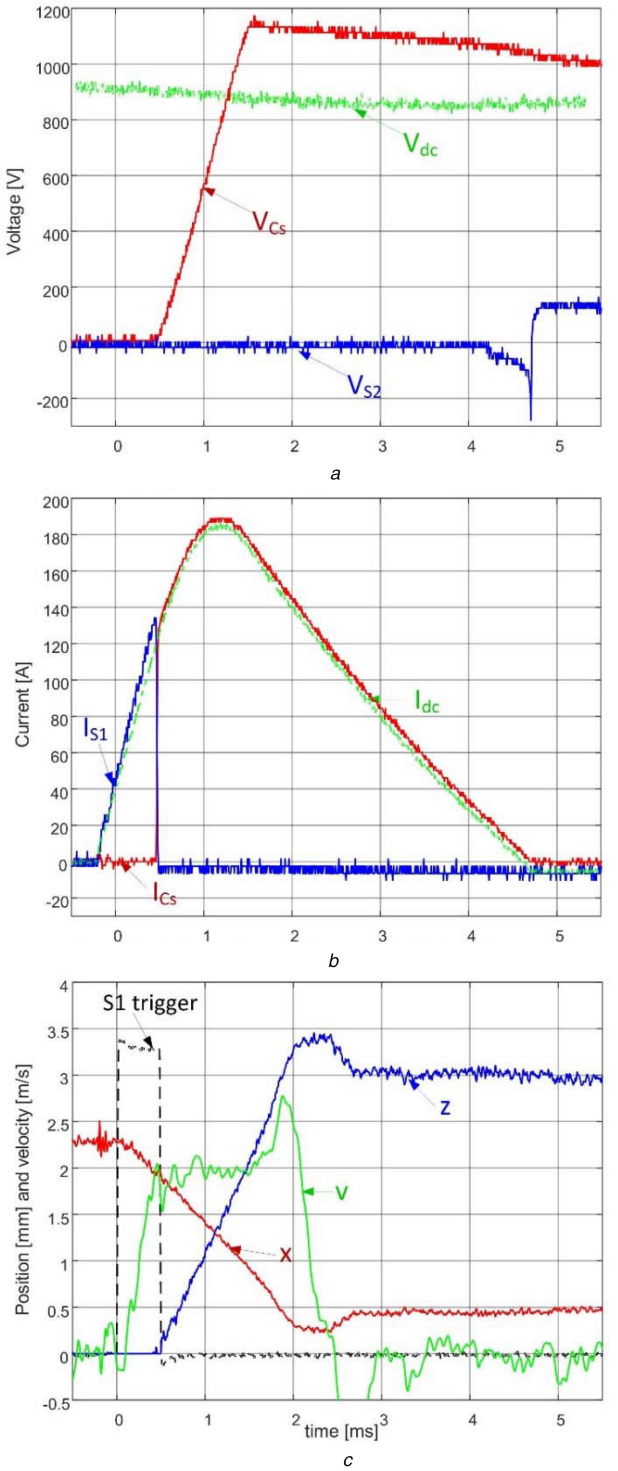

Fig. 7 *Experimental 900 V LC DC CB testing*

(a) Source (V_{dc}), Capacitor (V_{CS}) and switch S_2 (V_{S2}) voltages, ***(b)*** load (I_{dc}), capacitor (I_{Cs}) and switch S_1 (I_{S1}) currents, ***(c)*** S_1 contact position (x), gap distance (z) and velocity (v)

that the contacts separate when the DC current reduces to a low value, just before the first zero-crossing. It is seen that S_2 produces some arcing on voltage V_{S2} which lasts between 4 and 4.5 ms, at low voltage and low (20 A) current. The final voltage increase across S_2 (to around 150 V which is difference between arrester and DC supply voltage.) indicates successful interruption.

Fig. 7*c* shows the full switch contact position trajectory, and it also shows that the contact separation velocity is around 2 m/s.

The experimental LC DC CB is using the same test system, same disconnector and control as the reported hybrid DC CB [22], to enable comparison. However in [22] the current peaks at much

Table 2 Assumed parameters of the 320 kV, LC DC CB

Parameter	Value	Parameter	Value
V_{dc}	320 kV	overlap, OL	30 mm
I_{dcn}	2 kA	dielectric stress (SF6)	5 kV/mm
t_{max}	2 ms	separation, Z_{max}	96 mm
L_{dc}	200 mH	arrester, SA	490 kV
C_s	13 μF	—	—

higher value of 500 A which is the consequence of 2 ms waiting time for disconnector to fully open.

6 Evaluation of 320 kV series LC DC CB

6.1 320 kV series LC DC CB design

The LC DC CB concept has not been proven on high voltage hardware. This section gives only estimate of parameters and performance for a 320 kV LC DC CB in order to evaluate if there would be a possible benefit of scaling this topology to 320 kV. The design will be based on the principles in previous sections, and on the available 320 kV components. A complete model is developed in PSCAD, and the main parameters are given in Table 2.

S_1 can be presumed as (2 ms) SF6 disconnector which is demonstrated at 320 kV [7, 14] and a similar technology is used in [15]. Assuming 480 kV voltage stress and further 50% margin, the gap distance in the SF_6 disconnector is $z_{max} = 96$ mm. If contact travel time after separation is 1.6 ms, considering some breaking time, then average contact separation velocity is 66 m/s. The highest speed for contact operating rod is around 10–20 m/s because of mechanical limitations [12, 13]. Therefore in practice multiple contact breaking points are mounted on a single rod. As an example, speed of operating rod is only 16 m/s if 4 contact pairs are used, however the gap distance and velocity remain as in a single-contact case.

The value of $L_{dc} = 200$ mH is adopted in order to give sufficiently low initial current $I_{dc0} = 3.43$ kA, which helps to limit the peak fault current below 4.5 kA to avoid blocking a converter that is protected. The total protection time to trip signal is 0.35 ms, which is more than adequate for local protection methods, like those based on voltage derivative [23], and gives $I_{dc} = 2.6$ kA at the trip instant. The acceleration time for contacts is shorter than the time to separation which is assumed to be 0.55 ms considering studies in [13].

The condition (10) results in C_s>7.8 μF, condition (14) gives C_s>6.9 μF, while the condition (15) gives C_s>8 μF. To provide 60% safety margin $C_s = 13$ μF is selected. This would be initial theoretical assumption, which has not been verified.

The AC switch S_2 is assumed as vacuum interrupter which opens in 8 ms, in line with 70 kV installed units reported in [5]. Series connection of multiple units might be required.

6.2 PSCAD model

A detailed dynamic model for contact trajectory of the switch S1 is developed (Thomson coils, driving circuit, mechanical system) as described in [13]. The arcing is not occurring in S_1 in normal operation and therefore arc model is not essential. To simulate a possible dielectric breakdown, which would imply permanent failure of this DC CB, S_1 contact resistance R_{S1} is made:

$$R_{S_1} = \begin{cases} 0.002\,\Omega, & v_{CS} \geq v_{br} \\ 10^9\,\Omega, & v_{CS} < v_{br} \end{cases} \quad (17)$$

The modelling of DC circuit breaker follows methods described in [24]. A fixed 320 kV DC source is used and DC fault is represented with a 0.1 Ω resistance.

6.3 Simulation results

Fig. 8 shows the DC fault clearing simulation results, where the time instants are noted as in previous sections:

- $t_f = -0.35$ ms – DC fault,
- $t_0 = 0.0$ ms –fault detected, S_1-trip signal, ($I_{dc} = 2.6$ kA),
- $t_{sep} = 0.55$ ms – contact separation, $x = 15$ mm, $z = 0$ mm,, ($I_{dc} = 3.4$ kA),
- $t_{Idcp} = 1.65$ ms –peak current, $V_{Cs} = 320$ kV, $I_{dcp} = 4.4$ kA,
- $t_{max} = 2.2$ ms –maximum gap, $V_{Cs} = 480$ kV, z = 96 mm,
- $t_{S2} = 7.5$ ms – S_2 opens, $I_{dc} = 0$, $V_{Cs} = 430$ kV

In Fig. 8*a* it is seen that V_{br}>V_{Cs}, which ensures current commutation to C_s without arcing. The voltage rises while contacts are moving, and it is limited to 480 kV by the arresters. In Fig. *8b*, the peak fault current rises to 4.4 kA, which is just below typical blocking threshold for 2 kA converter IGBTs (around 2.5 pu). Fig. 8*c* illustrates that S_1 current commutates fully to capacitor at $t_{sep} = 0.55$ ms. Fig. 8*d* shows contact position x, separation distance z and velocity v.

6.4 Comparisons with hybrid and mechanical DC CB

In order to enable initial evaluation, a model for 320 kV hybrid DC CB [7] and 320 kV current injection mechanical DC CB [5] are also developed. In all 3 models, the same V_{dc}, L_{dc} and energy absorbers are used. The trip signal is at the same instant and therefore the current magnitude at the trip instant ($t = 0$) is identical. The resonant circuit components (L_p and C_p) for mechanical DC CB are calculated assuming 2.6 kHz resonant frequency [5], and they are shown for completeness.

Table 3 shows comparisons according to expected performance of LC DC CB (not confirmed experimentally). Comparing with hybrid DC CB, it is seen that LC DC CB would be marginally faster and has noticeably lower peak current and energy dissipation. More importantly, LC DC CB has only mechanical components and therefore cost is expected to be lower. While hybrid DC CB requires a valve hall and active cooling system, LC DC CB can be built as a simple outdoor unit.

Comparing with mechanical DC CB, it is seen that peak current and energy dissipation would be significantly (4 and 10 times respectively) lower. The mechanical DC CB also has considerably longer DC voltage recovery time and the final DC current interruption time. The LC DC CB may require similar total component costs as mechanical DC CB. LC DC CB requires a capacitor of $C_s = 13$ μF, which is four times higher than the resonant capacitor $C_p = 3.3$ μF in mechanical DC CB. Nevertheless, it is seen in Table 3 that the size of energy absorbers will be substantially lower (10 times). In terms of reliability and failure modes, LC DC CB may also have advantages. If mechanical DC CB fails to clear fault at the first zero-crossing, the DC current continues to rise and there are few subsequent zero-crossing opportunities. With LC DC CB, the current is AC with magnitude which is lower and stays constant in all subsequent cycles.

Table 4 compares the capacitors for LC and mechanical DC CB. The capacitance is 4 times larger with LC DC CB, but the peak current and frequency are substantially lower. These are important parameters that determine overall capacitor volume, since they have lower voltage rating for higher frequency.

Surge arresters are used with 320 kV LC DC CB tests in Fig. 8. If they are not used, the current can be interrupted, but the maximum voltage would reach 830 kV. This would bring savings in energy absorber costs, but C_s size would increase because of higher insulation level, and may not be acceptable for other HVDC components. Energy dissipation reduces as voltage increases, and further optimisation will be required.

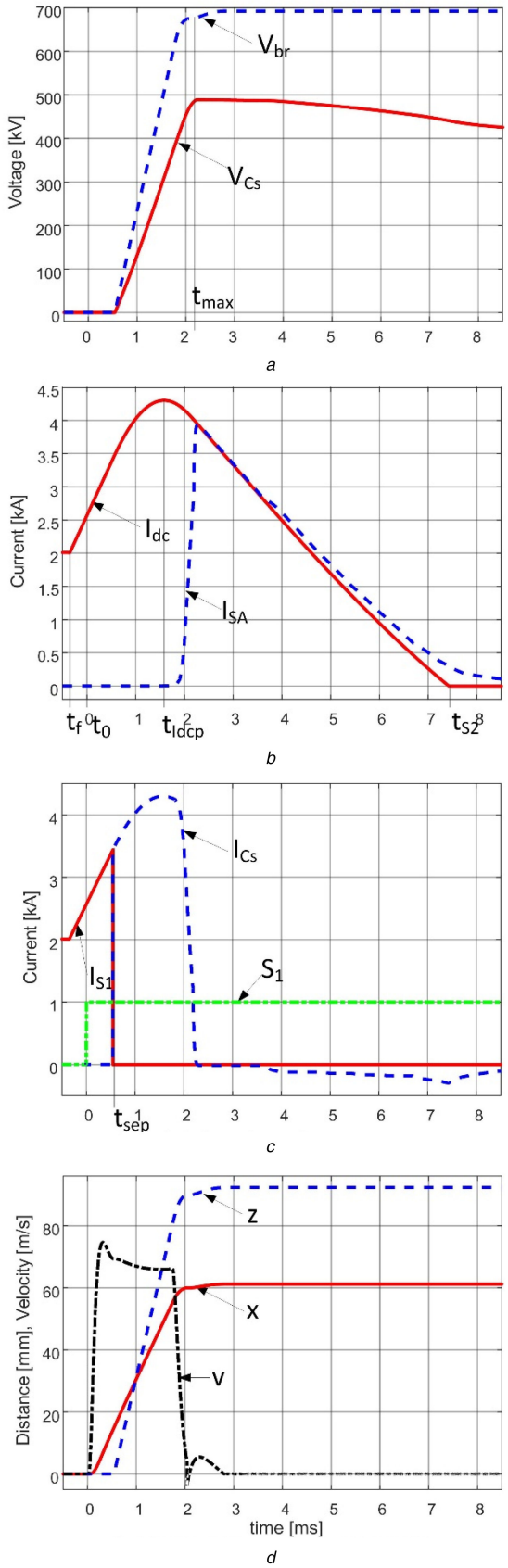

Fig. 8 *Simulation responses for 320 kV LC DC CB*
(a) Capacitor and contact withstand voltages, ***(b)*** Load and arrester currents, ***(c)*** Switch S_1 and capacitor currents, ***(d)*** Switch S_1 contact position and velocity

7 Conclusion

The article proposes a mechanical DC CB based on a series LC circuit (LC DC CB). It requires one fast disconnector, a fast AC Circuit breaker, an inductor and a capacitor, and therefore the cost is expected to be low and comparable with other mechanical DC CBs. It is illustrated that this DC CB converts DC current into AC, which will always have zero-current crossings and hence simple AC CBs are employed for the final interruption. The current commutation into a capacitor when disconnector opens is analysed and it is derived that analytical conditions exist to enable successful commutation.

Experimental results on a 900 V laboratory prototype DC CB illustrate successful DC fault clearing. A very good commutation of 130 A current is observed and clearing of 190 A peak DC fault current is demonstrated.

A detailed PSCAD model for 320 kV DC CB is developed and DC fault clearing is demonstrated, although no demonstrator is built at this voltage. Further comparisons with the existing 320 kV hybrid DC CB and mechanical DC CB illustrate significant possible benefits in terms of performance and costs. LC DC CB operates fast, and this leads to low peak current and energy

Table 3 Comparison of 320 kV series LC, hybrid and mechanical DC CB for identical initial conditions

	Parameters	Series LC DC CB	Hybrid DC CB [7]	Mech. DC CB [5]
initial conditions (identical for all)	V_{dc}	320 kV	320 kV	320 kV
	I_{dcn}	2 kA	2 kA	2 kA
	L_{dc}	200 mH	200 mH	200 mH
	t_f (protection trip)	0.35 ms	0.35 ms	0.35 ms
	I_{dcf} ($t = 0$)	2.6 kA	2.6 kA	2.6 kA
components	C_s (series capacitor)	13 μF	—	—
	C_p (resonant circuit)	—	—	3.3 μF
	L_p (resonant circuit)	—	—	1.1 mH
	T_2 (HV valve)	—	IGBT valve 480 kV, 16 kA	—
	LCS (LV valve)	—	IGBT valve 3 × 3, 10 kV, 6 kA	—
	S_1	fast disconnector	fast disconnector	fast vacuum switch
	S_2	fast vacuum switch	vacuum switch	vacuum switch
	S_3 (resonant circuit)	—	—	fast vacuum switch
performance	V_{dcp}	489 kV	491 kV	507 kV
	t_{max} (V_{dcmax})	2.0 ms	2.0 ms	8.0 ms
	I_{dcp}	4.4 kA	5.8 kA	15.7 kA
	t_{IDCP} (I_{dcpeak})	1.65 ms	2.0 ms	8.0 ms
	E_s	5.7 MJ	9.7 MJ	66 MJ
	t_{S2} ($I_{dc} = 0$)	7.5 ms	9.3 ms	25.5 ms

Table 4 Comparison of capacitors for LC and mechanical DC CB

Parameter	LC DC CB	Mech. DC CB
C_s	13 μF	3.3 μF
V_c	489 kV	507 kV
I_p	4.4 kA	15.7 kA
f_p	99 Hz	2.7 kHz
t_c	5.5 ms	0.37 ms

dissipation. Adequate design could potentially achieve very low peak fault current.

8 Acknowledgments

This work was supported by the European Union's Horizon 2020 research and innovation program under grant No. 691714. The author is thankful to Mr R. Osborne from University of Aberdeen for help with the experimental studies.

9 References

[1] Jovcic, D., Ahmed, K.: '*High voltage direct current transmission: converters systems and DC grids*' (Wiley, Chichester, UK, 2015)

[2] CIGRE joined WG A3 and B4.34: 'Technical requirements and specifications of state of the art HVDC switching equipment'. CIGRE brochure 683, April 2017

[3] Franck, C.M.: 'HVDC circuit breakers: A review identifying future research needs', *IEEE Trans. Power Deliv.*, 2011, **26**, (2), pp. 998–1007

[4] Bachmann, B., Mauthe, G., Ruoss, E., *et al.*: 'Development of a 500 kV airblast HVDC circuit breaker', *IEEE Trans. Power Appar. Syst.*, 1985, **PAS-104**, (9), pp. 2460–2466

[5] Tahata, K., Oukaili, S., Kamei, K., *et al.*: 'HVDC circuit breakers for HVDC grid applications'. Proc. IET ACDC 2015 conference, Birmingham, UK, February 2015, pp. 1–9

[6] Shukla, A., Demetriades, G.: 'A survey on hybrid circuit-breaker topologies', *IEEE Trans. Power Deliv.*, 2015, **30**, (2), pp. 627–641

[7] Häfner, J., Jacobson, B.: 'Proactive hybrid HVDC breakers – A key innovation for reliable HVDC grids'. Proc. CIGRE 2011 Bologna Symp., Bologna, Italy, September 2012, pp. 1–7

[8] Grieshaber, W., Dupraz, J., Penache, D., *et al.*: 'Development and test of a 120 kV direct current circuit breaker'. Proc. CIGRÉ Session, Paris, France, August 2014, pp. 1–11

[9] National Grid UK: 'Electricity ten year statement', 2014, Apepndix E. Available at https://www.nationalgrid.com/uk/publications/

[10] Rajotte, R., Drouet, M.G.: 'Experimental analysis of a fast acting circuit breaker mechanism: electrical aspects', *IEEE Trans. Power App. Syst.*, 1975, **PAS-94**, (1), pp. 89–96

[11] Genji, T., Nakamura, O., Isozaki, M., *et al.*: '400 V class high-speed current limiting circuit breaker for electric power system', *IEEE Trans. Power Del.*, 1994, **9**, (3), pp. 1428–1435

[12] Wen, W., Huang, Y., Al-Dweikat, M., *et al.*: 'Research on operating mechanism for ultra-fast 40.5-kV vacuum switches', *IEEE Trans. on Power Deloivery*, 2015, **30**, (6), pp. 2553–2560

[13] Bissal, A.: 'Modeling and verification o ultrafast electromechnaical actuators for HVDC breakers'. PhD Theiss, KTH, Stockholm, 2015

[14] Skarby, P., Steiger, U.: 'An ultra-fast disconnecting switch for a hybrid HVDC breaker – a technical breakthrough'. Proc. CIGRÉ Session, Alberta, Canada, September 2013, pp. 1–9

[15] Grieshaber, W., Dupraz, J., Penache, D., *et al.*: 'Development and test of a 120 kV direct current circuit breaker'. Proc. CIGRÉ Session, Paris, France, August 2014, pp. 1–11

[16] Rigden, J.S.: '*Macmillan encyclopedia of physics*' (Simon & Schuster, New York, NY, USA, 1996)

[17] Hedayati, M., Jovcic, D.: 'Low voltage prototype design, fabrication and testing of ultra-fast disconnector (UFD) for hybrid DCCB'. CIGRE B4 Colloquium, Winnipeg, October 2017

[18] Lopez-Roldan, J., Irwin, T., Nurse, S., *et al.*: 'Design, simulation and testing of an EHV metal-enclosed disconnector', *IEEE Trans. Power Deliv.*, 2001, **16**, (4), pp. 558–563

[19] Yanabu, S., Nishiwaki, S., Mizogushi, H., *et al.*: 'High current interruption by SF6 disconnecting swicthes in gas insulating switchgear', *IEEE Trans. Power Appar. Syst.*, 1982, **PAS-101**, (5), pp. 1105–1114

[20] Wayne Beaty, H., Fink, D.G.: '*Standard handbook for electrical engineers*' (McGrawHill, New York, NY, USA, 2013)

[21] Jovcic, D., Hedayati, M.H.: 'DC chopper based test circuit for high voltage DC circuit breakers'. IET ACDC Power Transmission, Manchester, February 2017

[22] Hedayati, M., Jovcic, D.: 'Reducing peak current and energy dissipation in hybrid HVDC CBs using disconnector voltage control', *IEEE Trans. Power Deliv.*, 2018, **33**, (4), pp. 2030–2038

[23] Sneath, J., Rajapakse, A.: 'Fault detection and interruption in an earthed HVDC grid using ROCOV and hybrid DC breakers', *IEEE Trans. Power Deliv.*, 2016, **31**, (3), pp. 973–981

[24] Lin, W., Jovcic, D., Nguefeu, S., *et al.*: 'Modelling of high power hybrid DC circuit breaker for grid level studies', *IET Power Electron.*, 2016, **9**, (2), pp. 237–246